Paper FG-24

Discrete element study of liquid-solid slurry flows through constricted channels

Micheline ABBAS[1], Martin Van der HOEF[2], Onno BOKHOVE[3] and Hans KUIPERS[4]

1: Dept. of Fundamentals of Chemical Reaction Engineering, Twente University M.E.Abbas@utwente.nl
2: Dept. of Fundamentals of Chemical Reaction Engineering, Twente University m.a.vanderhoef@utwente.nl
3: Dept. of Applied Mathematics, Twente University o.bokhove@utwente.nl
4: Dept. of Fundamentals of Chemical Reaction Engineering, Twente Universityj.a.m.kuipers@utwente.nl

Abstract Discrete element model is used to simulate the flow of liquid-granule mixtures in an inclined channel containing a linear contraction. All the relevant particle/particle and particle/fluid interactions are included in the numerical model. The presence of the contraction induces different steady morphologies of the solid phase or the mixture depending on whether closed or open channels are used. These flows behave quite differently depending on the upstream Froude number and the contraction size ratio. The model is first validated by comparing with the existing results for dry granular (glass particles) chute flows (Vreman et al., 2007). Then simulations of a chute of glass particles in water flowing in a closed channel are compared to the dry granular case. With the same solid flux at the inlet, the hydrodynamic forces in the liquid-solid mixture induce higher particle solid volume fractions in the part of the flow containing the solid phase. The streamwise particle velocity (resp. depth of the solid phase) has the same evolution along the channel with smaller (larger) values than in the dry granular flow case.

Keywords: Fluid-particle flow, Discrete Particle Model, chute flows,

1. Introduction

We study the behavior of slurry flows through a constriction. These concentrated liquid-solid mixtures are found in natural flows like mud slides initiated by heavy rainfall on eroded mountain sides. Also in industrial applications slurry flows are encountered for instance in pipeline transportation, where it is important to identify and control bottlenecks influence on production lines.

Chute flows are driven mainly by gravity and they are typically shallow. They are classified according to the Froude number Fr which is the ratio of the inertial to gravitational forces, and can be viewed as the hydrodynamic equivalent of the Mach number for gas flows. Simplified hydraulic theories for one-phase shallow flows based on depth and cross-averaged approximations have been compared to experiments with both water (Akers and Bokhove 2008) and with dry granular material (Vreman et al. 2007). The influence of bottleneck on the flow is different, depending on whether the upstream flow is sub or supercritical (Fr<1 and Fr>1 respectively), and on the width of the contraction relatively to the width of the chute. One may find bores/shocks both steady or moving upstream, oblique waves in the contraction, as well as a steady reservoir with a complex hydraulic jump in the contraction.

Multiphase shallow flows are far more complex. Depth-averaging techniques are commonly used to simplify the three dimensional equations (Rhebergen et al., 2009). However these models rely heavily on closures, especially the stress parametrizations. We intend to use in this study the simulation of discrete elements where the solid elements in the flow are tracked individually. The strong point of this method is that, once validated by direct comparison with the experiments, it allows for calculating physical quantities that are difficult or impossible to measure in experiments like the stress distribution in the

system.

A version of the Discrete Element Model - usually used for gas-solid fluidized beds (Hoomans et al. (1996), Van der Hoef et al.(2006)) - is modified to allow for simulation of liquid-particle flows through a channel containing a linear contraction. The geometry of the simulated channel and its orientation with respected to the gravity are represented in Fig. 1. The inclination angle of the chute is chosen in such a way that when the contraction is removed, the flow is as uniform as possible (no visible surface or density waves).

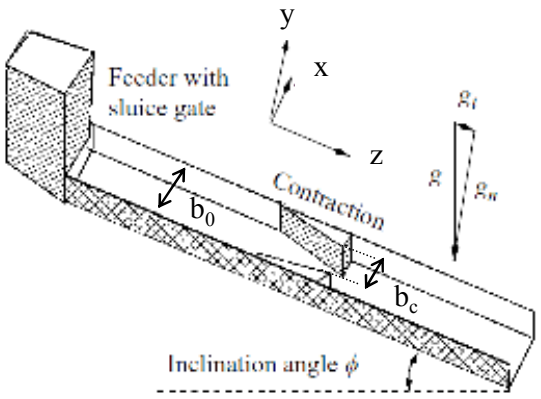

Fig. 1
Channel geometry. **g** is the gravity acceleration.

The objective of this paper is to make a first assessment of the ability of the discrete particle model to study the slurry flows, and to have an idea on the influence of the contraction on the two phase flows. We stress that it is the first study that includes the complete interactions between the liquid and solid particles in the discrete element model.

2. System equations

2.1 Particle equations

The motion of each spherical particle is calculated from the second Newton law of motion

$$m_p \frac{dv_p}{dt} = F_P + F_D + F_G + F_{pp} + F_{AM} + F_{lub} \quad (1)$$

All the relevant forces applied on a solid particle in a liquid phase are taken into account. The forces appearing on the right hand-side are due to pressure, drag, gravity, particle-particle collision, added mass and lubrication effects. The drag correlation is taken from the work of Beetstra et al. (2006), which is valid for a wide range of Reynolds numbers and porosities. The lubrication force is based on the Stokes interaction between a pair of particles that are close together (Nguyen and Ladd, 2002).

Particle-particle collision dynamics are described by collision laws, which account for energy dissipation due to the non-ideal particle interaction by means of the empirical coefficients of normal and tangential restitution, and the coefficient of friction. The particle collisions are represented by a spring/dash-pot system following the soft-sphere model. Small overlapping between two particles is allowed (less than 2% of the average particle radius).

2.2 Liquid equations

The flow field of the liquid phase (density ρ_f and flow velocity $\boldsymbol{u}$) is computed from the volume-averaged Navier-Stokes equations given by

$$\rho_f \frac{\partial \varepsilon}{\partial t} + \rho_f \nabla \cdot (\varepsilon \mathbf{u}) = 0 \quad (2)$$

$$\rho_f \frac{\partial (\varepsilon \mathbf{u})}{\partial t} + \rho_f \nabla \cdot (\varepsilon \mathbf{u}\mathbf{u}) = -\varepsilon \nabla p - \nabla \cdot (\varepsilon \boldsymbol{\tau}_f) - \mathbf{S}_p + \varepsilon \rho_f \mathbf{g}$$

The viscous stress tensor $\boldsymbol{\tau}_f$ is assumed to obey the general form for a Newtonian fluid (Bird et al. 1960). p is the fluid pressure field. The particle influence in the fluid equations appears through the fluid volume fraction ε. It is calculated using the local volume occupied by the particles in the different fluid cells. Two-way coupling is achieved via the momentum sink/source term $\boldsymbol{S}_p$ which includes the fluid-particle drag force and the added mass force contributions. Details of the treatment of the inter-phase momentum change due to the drag force can be found in Hoomans et al. (1996). The added mass contribution is implemented in

$\boldsymbol{S}_p$ in the same way as the drag force. It also contributes to increase the particle apparent mass. Note that the lighter the particles are the more relevant this contribution becomes.

Fixed Eulerian mesh is used to solve the Navier-Stokes equations of the fluid. Eq. (2) is valid provided that the particle volume fraction is less than 1. In our study, a fluid cell contains typically O(10) particles. Note that for liquid-solid flows, the fluid phase should be treated as incompressible, which requires a solution procedure that is slightly different from what is described in Hoomans et al. (1996) and Van der Hoef et al. (2006).

3. Results in closed channels

A linear contraction is introduced inside the channels as shown in Fig. 2. The walls of the contraction are represented by layers of fixed particles. Note that this modeling approximation induces wall roughness which increases when the size of the particles increases. It also induces wall permeability in the liquid-solid simulations which can be reduced, however, by replacing one layer of particles by multiple layers.

3.1 Dry granular flow

Before performing simulations of granules in liquid, we first validated the particle model by running simulations of dry granular flow of glass spherical particles in a constricted channel. The effect of the contraction on the dry granular flow has been extensively discussed in the work of Vreman et al. (2007) comparing experiments, discrete element simulations and theoretical analysis. The simulation parameters that we used are chosen such to match the experimental conditions of granular chute flows as studied by Vreman et al. (2007). Table 1 summarizes the different relevant parameters with regard to the box, particles, flow, time step, etc. The particles are introduced with an average streamwise velocity (in the z direction) of U_{in}=17cm/s, and with a 2% velocity fluctuations in the 3 directions.

Channel	ϕ=19°	Sluice gate 1.1cm	$\begin{pmatrix} x \\ y \\ z \end{pmatrix} = \begin{pmatrix} 13 \\ 1.8 \\ 70 \end{pmatrix}$ cm
Particles	d_p=1mm	N_p=3.510^5	ρ_p= 2.5g/cm^3
Collisions	e_n=0.97 β=1	k_n=16k_t= 100 N/m	μ=0.344
Contraction	L=20.4cm	b_c/b_0= 0.38	$d_w=d_p/2$
Flow rates	U_{in} = 17cm/s	Q_p=0.073 V_b/s	
Time	T = 8s	dt = 2.5 10^{-5}s	

Table 1
Parameters of the simulations with dry granular flow (corresponding to Fig. 3).

The contraction damps the flow and induces a non-homogeneous particle distribution in the system: steady shocks or large jumps in granular depth. The existence of these different states has been discussed as a function of the upstream Froude number and of the contraction size ratio b_c/b_0. The authors have found 4 different steady states depending on the dimensionless numbers.

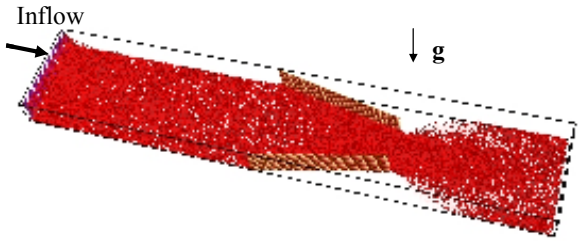

Fig. 2
Dry granular flow after reaching steady state in a constricted channel. The simulation parameters are according to Table 1.

Statistical characterization of the flow is performed through averaged quantities. Once the steady state is reached, the time average of a quantity φ (like the solid phase velocity) is defined in a cell *i* as following:

$$\langle \alpha\varphi \rangle_t = \frac{\pi d_p^3}{6\tau V_{cell}} \int_{t-\tau}^{t} \sum_i \varphi_i dt \qquad (3)$$

where the sum is taken over all particles with xyz-coordinates of their centers inside a local cube of volume V_{cell} with ribs $\Delta x=\Delta z=2d_p$ and Δy=1mm. α is the solid volume fraction. τ is the averaging time. The time-average of φ is

defined as $[\varphi]_t = \langle \alpha\varphi \rangle_t / \langle \alpha \rangle_t$. The cross-sectional average of φ is calculated by averaging across the width of the flow. The local depth of the flow is defined from the highest local particle in the y direction.

Fig. 3 shows a comparison of the cross-sectional average of the solid volume fraction and of the flow depth. Our results follow the same trend as the simulation results of Vreman et al. (2007) which were successfully compared to experiments in similar conditions. The small deviation in the results is due mainly to the way we represent the contraction walls, and how the particles are introduced at the channel inlet.

a)

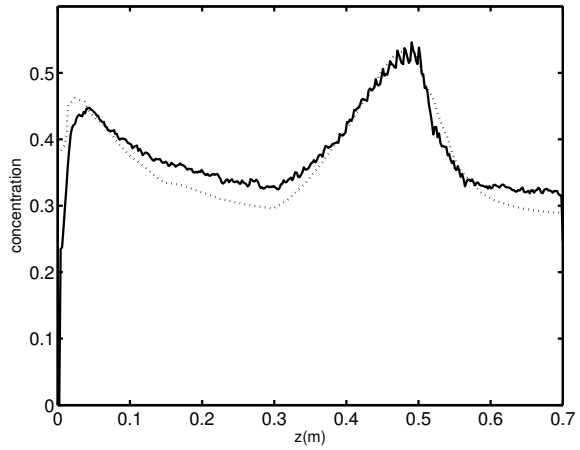

b)

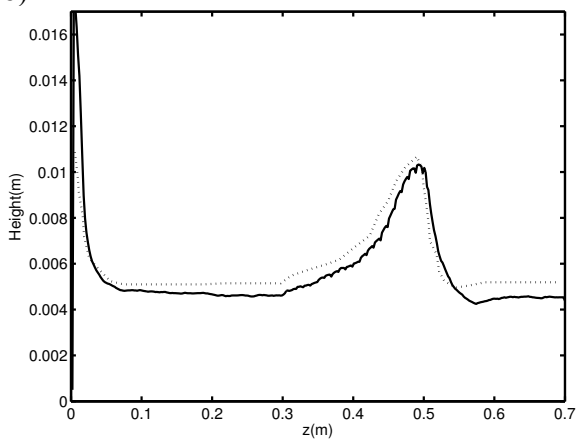

Fig. 3
Evolution of cross-sectional average of a) solid volume fraction and b) flow depth in the flow direction (z) in dry granular chute flow. Solid line: results of present study. Dotted line: Vreman et al. (2007).

3.2 Liquid-particle flow

In order to have a first impression on the effect of the liquid in the chute flow, we performed identical simulations for two different chute flows: dry granular and liquid-solid. The parameters are the same as in Table 1. However the box size is smaller (details are given in Fig. 4). In the liquid-solid case the particles are introduced in a channel full of water. The equations for the liquid are solved using no-slip boundary conditions at the channel walls. Of course the hydrodynamic forces play an important role damping the motion of particles. Fig. 4 shows that the particle behavior in the presence of liquid is very different from the "dry" case. Downstream the nozzle, the angle in which solid phase is flowing is smaller. In concentrated zones, particle contacts are important and the bulk behavior is controlled by particle-particle interactions. However in zones with concentration gradient hydrodynamic interactions are the driving forces.

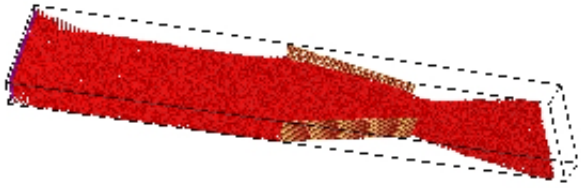

Fig. 4
Chute flow of glass particles in water in a closed channel. Each wall of the contraction is replaced by one layer of particles. The simulation parameters are similar to Table 1. Dimensions of the box: (6,1.8,32) cm^3 – b_c/b_0=0.417 – Q_p=0.082 V_b/s.

To quantify the difference between the dry and wet cases, the statistical behaviors are compared in both cases. The profiles of cross-averaged concentration and flow depth are shown in Fig. 5. In the liquid-solid flow, the glass particles are sedimenting to the bottom of the bed.

It is clear from Fig. 5 that at the same flux of particles, larger solid volume fractions and lower particle streamwise velocities are found in the liquid-solid flows over the entire domain. The large jump in concentration appearing in the granular flows disappears in the liquid-solid case. In the liquid-solid flows, thicker reservoirs with a large jump in the bed depth

are formed in the vicinity of the contraction. The local Froude number is calculated using $\mathrm{Fr} = \mathrm{U}/\sqrt{\mathrm{gh}}$ where U and h are respectively the local velocity and height of the solid particle flow. The Froude number decreases from 2.5 (upstream flow) to 0.96 (end of the contraction) in the dry granular flow whereas it decreases from 1.4 to 0.35 in the liquid-solid flow case. Hence the flow of solid phase hardly reaches the subcritical limit in the dry granular case, which is in clear contrast with the liquid-solid chute flow which becomes strongly subcritical (in the contraction zone) even for an inclination angle as high as 19°. From the profiles of Fig. 5 we can only deduce that they vary in a smoother way in the liquid-solid flow than in the dry granular one. However, a complete dimensionless analysis for the liquid-solid mixture in terms of the Froude number is not meaningful since the system is not a real open channel.

It is also obvious that these results are valid for particles much heavier than the water. When the particle density is close to the water density, they will not sediment at the bottom of the bed, but may interact with the upper part of the channel, and hence the curves of Fig. 5 are not valid anymore.

We want to stress that those results should be regarded as preliminary, and are to be followed by a far more extensive analysis in terms of the different dimensionless quantities that play a role in the system, among them the Froude, Reynolds and Stokes numbers for quantifying the influence of the gravity wave, viscosity and particle inertia effects.

4. Conclusions and outlook

A discrete element model has been adapted for liquid-solid chute flow simulations in a constricted channel. In the dry granular chute flow case, the model was compared to the work of Vreman et al. (2007) in a good accordance. A test case was carried on liquid-solid chute flows in a closed channel. The influence of the contraction on the liquid-solid flow was shown to be different than that in the dry granular case. For the case studied in section 3.2, the following difference was found in the liquid -

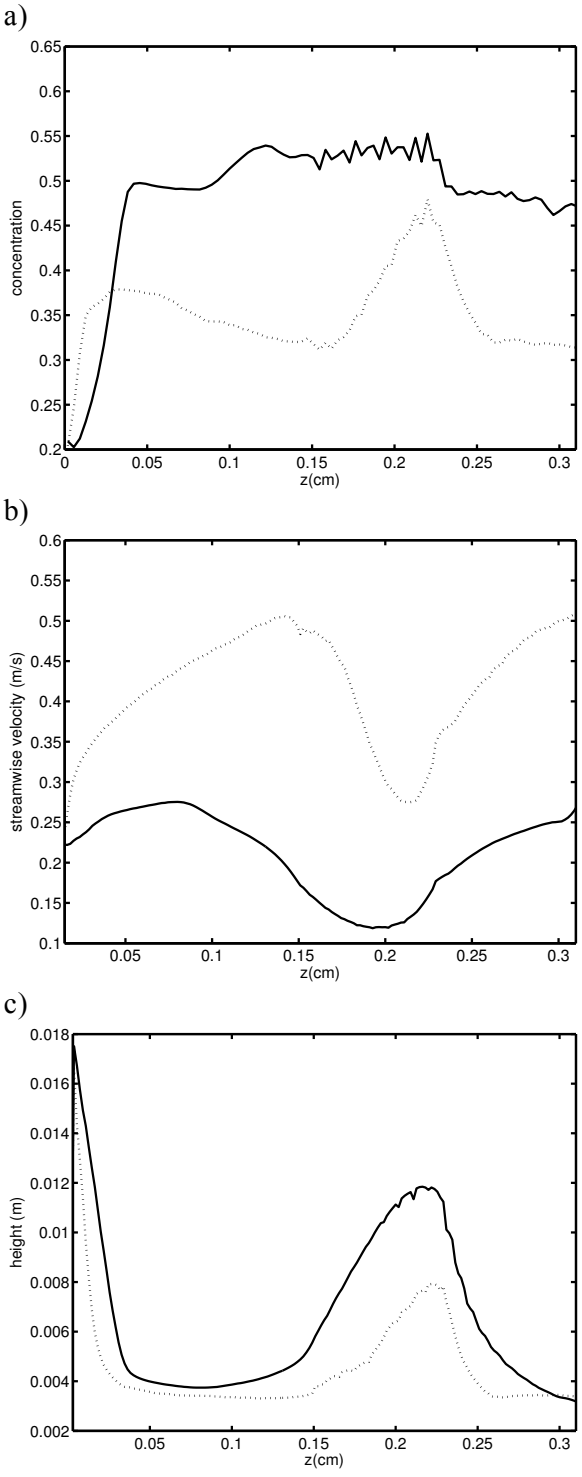

Fig. 5
Evolution of cross-sectional average of a) solid volume fraction and b) flow depth c) streamwise particle velocity in the flow direction (z). The dry granular (dashed lines) and the liquid-solid (solid lines) flows are compared.

solid case concerning the solid phase: higher concentration and smaller streamwise velocity in the whole bed, and thicker reservoir in the upstream neighborhood of the contraction.

In parallel, experiments are carried out for a system of beads suspended in water in an open channel. However, experiments are performed in open channels, like most of the slurry flows do. A higher credibility of the model compared to the experiments will be conditioned by implementing the free surface effect. We intend to account for this effect using two methods. The first method assumes geometric linearization of the free surface. A modification of the boundary condition allows for adding the kinematic and dynamic boundary conditions on the free surface in a simplified way. The second method is more direct and consists of combining the Volume of Fluid with the Discrete Particle Model.

Comparison of the numerical and experimental results (on a 1 to 1 scale) will allow us to improve the modeling of the constitutive relations and frictional parameterizations as already used in depth-averaged models developed for shallow two-phase flows (Rhebergen et al., 2009).

5. Nomenclature

b_0 : Channel width [m]
b_c : Smallest contraction width [m]
d_p : Particle diameter [m]
dt : Time step [s]
d_w :Diameter of particles forming the contraction walls [m]
e_n : Normal particle-particle and particle-wall restitution coefficient
F : Force applied on particle [N]
k_n : Normal spring stiffness (collision)
k_t : Tangential spring stiffness (collision)
L : Length of the contraction wall [m]
m_p : Particle mass
N_p : Number of particles
p : Fluid field pressure [Pa]
Q_p : Volume flow rate of particles [m^3/s]
u : Fluid field velocity [m/s]
U_{in} : Fluid velocity at the inlet [m/s]
V_b : Volume of the channel [m^3]
v_p : Particle velocity [m/s]

β : Tangential particle-particle and particle-wall restitution coefficient
ε : Fluid volume fraction
ϕ : Chute inclination angle
μ : Friction coefficient
ρ_p : Particle density [kg/m^3]
ρ_f : Fluid density [kg/m^3]

6. References

Beetstra R., Van der Hoef M. A., and Kuipers J. A. M., 2006. Drag Force of Intermediate Reynolds Number Flow Past Mono- and Bidisperse Arrays of Spheres. AICHE, 53 489-501

Bird, R.B., Stewart,W.E., Lightfoot, E.N., 1960. Transport Phenomena. Wiley, New York, pp. 79.

Akers B. and Bokhove O. 2008., Hydraulic flow through a channel contraction: Multiple steady states. Physics of Fluids, 20:056601–1:15.

Hoomans B.P.B., Kuipers J.A.M., Briels W.J., Van Swaaij W.P.M., 1996. Simulation of bubble and slug formation in a two-dimensional gas-fluidized bed: a hard-sphere approach. Chemical Engineering Science, 51:99-118.

Nguyen N.-Q. and Ladd A. J. C., 2002. Lubrication corrections for lattice-Boltzmann simulations of particle suspensions. Physical Review E 66 046708-1:12

Rhebergen S., Bokhove O., and Van der Vegt J.J.W., 2009. Discontinuous galerkin finite element method for shallow two-phase flows. submitted to Comput. Methods Appl. Mech. Eng., 198:819-830.

Van der Hoef, M.A., Ye, M., Van Sint Annaland, M., Andrews, A.T., Sundaresan S., Kuipers J.A.M., 2006. Multiscale modelling of gas-fluidized beds. Adv. Chem. Eng. 31: 65-149.

Vreman A.W., Al-Tarazi M., Kuipers J.A.M., Van Sint Analand M., and Bokhove O., 2007. Supercritical shallow granular flow through a contraction: experiment, theory and simulation. J. Fluid Mech., 578:233–269.